Photochemistry of Pentacarbonyl(cyclohepta-1,3,5-triene-7-carbonyl)manganese and Pentacarbonyl(σ-cycloheptatrienyl)rhenium in Frozen Gas Matrices at *ca.* 12 K: Infrared Spectroscopic Evidence for Carbon Monoxide Ejection with Concomitant Polyene Ring Hapticity Changes

Andrew K. Campen, Ramaier Narayanaswamy, and Antony J. Rest *
Department of Chemistry, The University, Southampton SO9 5NH

Infrared spectroscopic evidence, including ^{13}CO labelling and energy-factored force-field fitting, is presented to show that once a CO ligand has been photochemically ejected from $[Mn(C_7H_7CO)(CO)_5]$ to yield $[Mn(\sigma\text{-}C_7H_7)(CO)_5]$ *via* a 16-electron species, $[Mn(C_7H_7CO)(CO)_4]$, subsequent photolyses of $[M(\sigma\text{-}C_7H_7)(CO)_5]$ complexes (M = Mn or Re) leads to sequential formation of the 18-electron species $[M(\eta^3\text{-}C_7H_7)(CO)_4]$, $[M(\eta^5\text{-}C_7H_7)(CO)_3]$, and $[M(\eta^7\text{-}C_7H_7)(CO)_2]$ in Ar, CH_4, N_2, and CO matrices at *ca.* 12 K. The fact that no 16-electron species were observed prior to ring slippage even at such low temperatures indicated that such ring slips occur extremely readily or that they occur as a concerted process with CO ejection. The facility of the ring-slippage process was demonstrated by the failure of intermediate species $[M(\sigma\text{-}C_7H_7)(CO)_5]$ and $[M(\eta^3\text{-}C_7H_7)(CO)_4]$ to undergo exchange with ^{13}CO in doped matrices or to take up a N_2 ligand when photolyses are carried out in nitrogen matrices. Exchange with ^{13}CO and substitution of CO by N_2 does, however, occur once the ring-slippage process is nearing completion for Mn affording $[Mn(\eta^5\text{-}C_7H_7)(^{12}CO)_n(^{13}CO)_{3-n}]$ and $[Mn(\eta^5\text{-}C_7H_7)(CO)_2(N_2)]$. The electronic spectra of $[Mn(\eta^7\text{-}C_7H_7)(CO)_2]$ shows vibrational splitting which indicates a symmetric structure, *cf.* $[Co(\eta^5\text{-}C_5H_5)(CO)_2]$, rather than a bent geometry. The photophysical and photochemical processes associated with the observed reactions are discussed.

The diamagnetism of organometallic complexes together with the 18-electron 'rule' allows the ready formulation of their structures. For example, $[Fe(C_{10}H_{10})(CO)_2]$ must contain both η^5- and σ-cyclopentadienyl ligands, *i.e.* the structure is $[Fe(\eta^5\text{-}C_5H_5)(\sigma\text{-}C_5H_5)(CO)_2]$, as confirmed by *X*-ray crystallography.[1] In the cases of larger polyenes, not all the C atoms of the polyene need be involved in bonding to the metal, *e.g.* $[Fe(C_8H_8)(CO)_3]$ and $[Co(C_7H_7)(CO)_3]$ are $[Fe(\eta^4\text{-}C_8H_8)(CO)_3]$[2] and $[Co(\eta^3\text{-}C_7H_7)(CO)_3]$,[3] respectively.

Organometallic complexes containing the cycloheptatrienyl ligand have been known for a considerable period of time but are nowhere as numerous as cyclopentadienyl complexes.[4] The hapticity of the C_7H_7 ligand ranges all the way through from σ to η^7, *e.g.* $[Re(\sigma\text{-}C_7H_7)(CO)_5]$,[4] $[Co(\eta^3\text{-}C_7H_7)(CO)_3]$,[3] $[Mn(\eta^5\text{-}C_7H_7)(CO)_3]$,[5] $[V(\eta^7\text{-}C_7H_7)(CO)_3]$,[6] and $[M(\eta^7\text{-}C_7H_7)(CO)_3]^+$ (M = Cr, Mo, or W).[7]

The variations in hapticities have two important consequences: (*a*) changes in the hapticity of a polyene provide a route, the so-called 'ring-slippage' route,[8] for substitution reactions at the metal by an associative mechanism;[9] (*b*) changes in hapticity may also be implicated in the fluxional behaviour of polyenes, the so-called 'ring-whizzers'.[10]

Studies of compounds capable of demonstrating a range of hapticities for the same metal afford, therefore, valuable insights into polyene–metal bonding and reactivity. Such compounds are the complexes $[M(C_7H_7CO)(CO)_5]$ (M = Mn or Re) which are known to yield $[Mn(\eta^5\text{-}C_7H_7)(CO)_3]$[5] and $[Re(\sigma\text{-}C_7H_7)(CO)_5]$[4] and a dimeric species on photolysis of the parent compounds, respectively (Scheme 1). A route to $[Re(\eta^5\text{-}C_7H_7)(CO)_3]$ (as a minor product) has been discovered *via* photolysis of $[Re_2(CO)_{10}]$ in the presence of C_7H_8.[11] The difference in the products for Mn and Re has been ascribed to the greater strength of the Re–C as compared to the Mn–C bond, *cf.* the dissociation energies of the M–C bonds in the

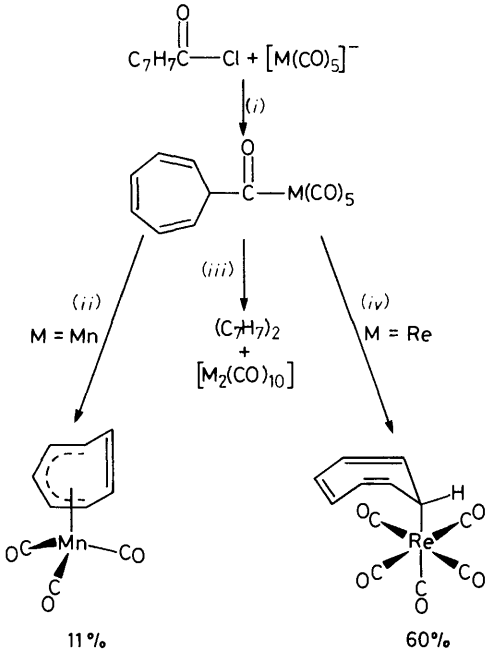

Scheme 1. The contrasting chemistry of $[M(C_7H_7CO)(CO)_5]$ (M = Mn or Re) upon u.v. photolysis in low-temperature solutions. (*i*) Tetrahydrofuran (thf), 20 °C; (*ii*) *hν*, −65 °C, Me_2CO; (*iii*) *hν*, room temperature (r.t.); (*iv*) *hν*, −78 °C, Me_2CO

$[M(CO)_5Me]$ complexes.[12,13] These studies strongly indicate that it is the weakness of the Mn–C single bond which precludes the isolation of $[Mn(\sigma\text{-}C_7H_7)(CO)_5]$ as a stable complex.

In order to investigate the changes in hapticity further, the

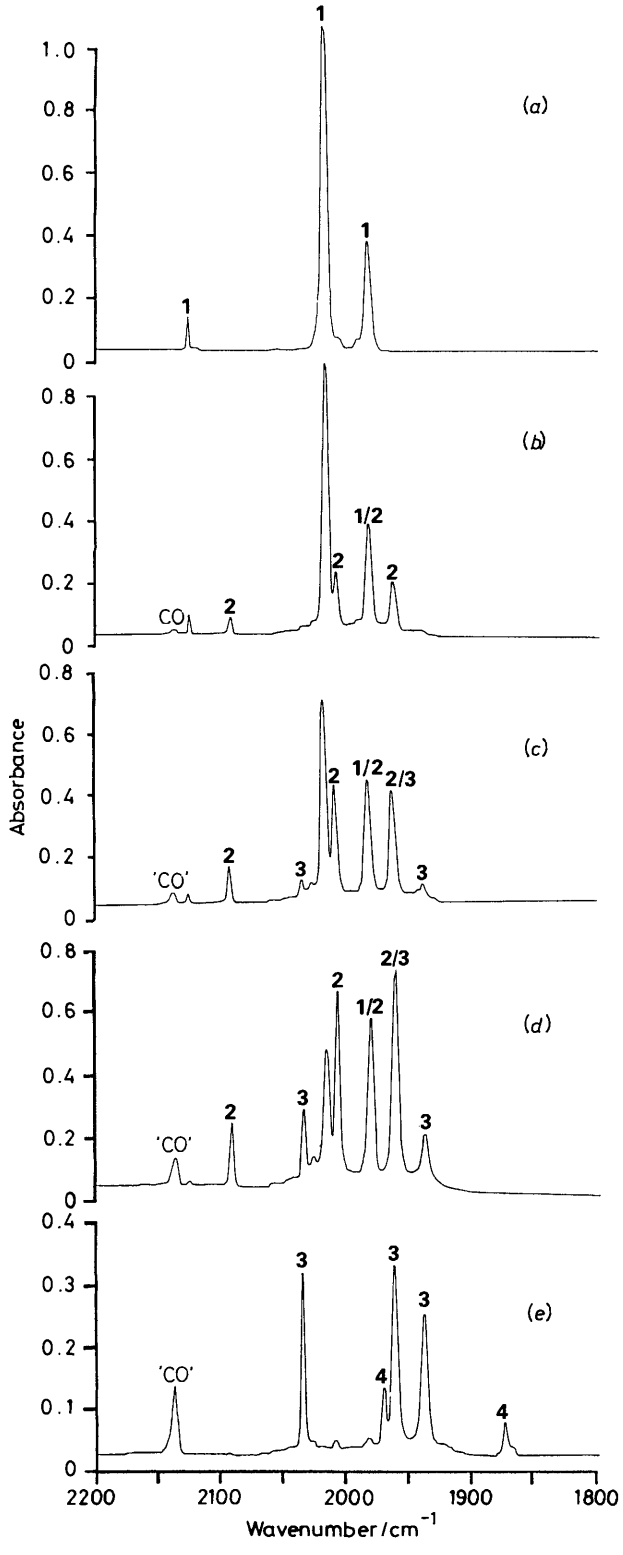

Figure 1. Infrared spectra (Nicolet 7199) (CO-stretching region) of $[Re(\sigma\text{-}C_7H_7)(CO)_5]$ and its photoproducts isolated at high dilution in an argon matrix: (*a*) starting spectrum, (*b*) 20 min, (*c*) 60 min, (*d*) 120 min, and (*e*) 240 min with filter A

complexes $[Mn(C_7H_7CO)(CO)_5]$ and $[Re(\sigma\text{-}C_7H_7)(CO)_5]$ were photolysed in Ar, CH_4, N_2, CO, and ^{13}CO-doped CH_4 matrices at *ca.* 12 K and the products characterised by i.r. and u.v.–visible spectroscopy.

Experimental

Details of the matrix-isolation equipment, the matrix gases, and the mercury arc lamp used for photolysis have been described elsewhere.[14] I.r. spectra were either obtained using a Nicolet 7199 Fourier-transform spectrometer performing at a quoted resolution of 1.0 cm^{-1}, also described previously,[14] or a Perkin-Elmer 983G grating spectrometer which was operated at a quoted resolution of 0.5 cm^{-1}.

U.v.–visible spectra were obtained using a Perkin-Elmer Lambda 7 spectrometer linked to a Perkin-Elmer 3700 data station, the latter facility allowing spectral subtractions and derivative spectra to be calculated.

Samples of $[Mn(C_7H_7CO)(CO)_5]$[5] and $[Re(\sigma\text{-}C_7H_7)(CO)_5]$[4] were kindly provided by Professors P. Hofmann and W. A. G. Graham, respectively. The former tended to decompose to $[Mn_2(CO)_{10}]$ and $(C_7H_7)_2$ which both needed pumping off prior to use. Matrix samples were prepared by the slow spray-on technique with samples held at specific temperatures {$[Mn(C_7H_7CO)(CO)_5]$ at 20 °C and $[Re(\sigma\text{-}C_7H_7)(CO)_5]$ at 25 °C} while co-condensing a large excess of the matrix gas.

Wavelength-selective photolysis was afforded using combinations of absorbing materials: filter A, $\lambda > 290$ nm, Pyrex disc (thickness 2 mm); filter B, $290 < \lambda < 370 > 550$ nm, quartz gas cell (pathlength 27 mm), containing Br_2 (200 Torr, *ca.* 2.7×10^4 Pa) + Pyrex disc (thickness 2 mm); filter C, $390 < \lambda$ 440 nm, Corion glass filter P70-400-S-1339; and filter D, $\lambda > 460$ nm, Corning glass filter 3385.

Results

(*i*) *Photolysis of* $[Re(\sigma\text{-}C_7H_7)(CO)_5]$ *isolated at High Dilution in* Ar, CH_4, *and* CO *Matrices at* ca. 12 K.—The i.r. spectrum of $[Re(\sigma\text{-}C_7H_7)(CO)_5]$ (**1**) isolated at high dilution in an argon matrix is shown in Figure 1(*a*). The spectrum reveals that the $Re(CO)_5$ fragment has a C_{4v} local symmetry, the band positions agreeing well with those reported by Heinekey and Graham[4] for the complex in cyclohexane solution. A lower symmetry in the matrix would have led to a lifting of the degeneracy of the *E* mode at 2 019.0 cm^{-1} resulting in four i.r. bands rather than the three observed. The lack of matrix splitting in argon and in carbon monoxide but not in methane* is supportive of the proposal by Heinekey and Graham[4] that the molecule exists either predominantly or exclusively in the quasi-axial conformation, a conclusion which was drawn from both the crystal structure and n.m.r. solution studies.

The solution u.v.–visible spectrum of compound (**1**) showed five absorptions (n-hexane) at 212 (ε = 36 000), 261 (ε = 5 100), 281 (ε = 5 100), 305 (shoulder, ε *ca.* 2 000), and 388 nm (ε = 2 600 $dm^3\ mol^{-1}\ cm^{-1}$) in reasonable agreement with the band positions and absorption coefficients quoted by Heinekey and Graham.[4]

Initial photolysis (20 min, filter A) at $\lambda > 290$ nm led to a decrease in the intensity of the i.r. bands attributed to (**1**) and the appearance of four new bands at 2 094.5, 2 010.5, 1 984.0 (overlapped with A_1 parent band at 1 984.5 cm^{-1}), and 1 966.0 cm^{-1} as well as a band at 2 137.0 cm^{-1} due to 'free CO' [Figure 1(*b*)]. Long-wavelength photolysis with a range of filters failed to produce any reversal.

Further photolysis with filter A (total 60 min) led to a continuing increase in the four bands associated with the initial photoproduct (**2**) and a concomitant decrease in those of (**1**), plus an increase in the band for 'free CO.' Three new weak bands

* Matrix splittings and band positions are commonly found to vary with matrices.[15,16]

Table 1. Infrared band positions (cm^{-1}) * for $[Re(\sigma\text{-}C_7H_7)(CO)_5]$ and its photoproducts in the terminal CO-stretching region in argon, methane, and carbon monoxide matrices

Complex	ν_{CO}	Ar	CH_4	CO
(1) $[Re(\sigma\text{-}C_7H_7)(CO)_5]$	A_1	2 127.0w	2 125.0w	2 119.0w
C_{4v}			2 019.0s	
	E	2 019.0vs	2 015.0vs	2 017.5s
			1 987.0w (sh)	
	A_1	1 984.5m	1 980.0s	1 977.0m
(2) $[Re(\eta^3\text{-}C_7H_7)(CO)_4]$	A'	2 094.5m	2 092.0m	2 089.5m
C_s	A'	2 010.5s	2 006.5s	2 005.5s
	A''	1 984.0s	1 981.0s	1 977.5s
	A'	1 966.0s	1 962.5s	1 956.0s
(3) $[Re(\eta^5\text{-}C_7H_7)(CO)_3]$	A'	2 037.0s	2 034.5s	2 034.0s
C_s	A''	1 964.5s	1 960.5s	1 958.5s
	A'	1 940.0m	1 935.5m	1 934.0m
(4) $[Re(\eta^7\text{-}C_7H_7)(CO)_2]$	A_1	1 972.0w	1 968.0w	1 968.0w
C_{2v}	B_1	1 874.0w	1 870.5w	1 864.5w

* Relative intensities: v = very, w = weak, m = medium, s = strong, and sh = shoulder.

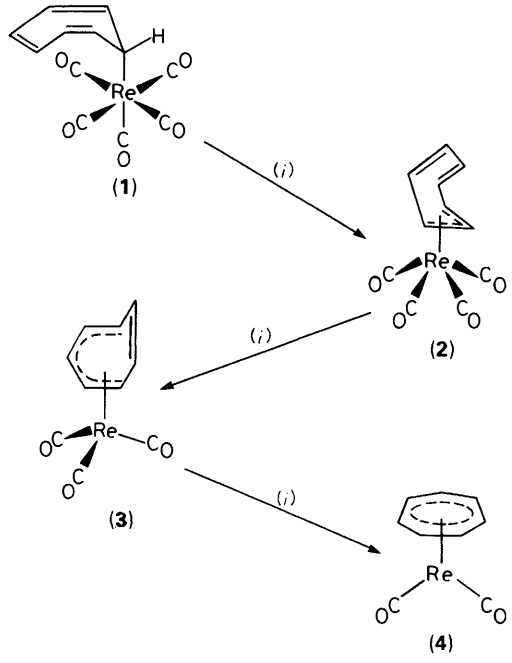

Scheme 2. The photoreactions of $[Re(\sigma\text{-}C_7H_7)(CO)_5]$ isolated at high dilution in various matrices at 12 K. (*i*) *hν*, −CO, filter A

also appeared at 2 037.0, 1 964.5 [overlapped with A_1 band due to (**2**) at 1 966 cm^{-1}], and 1 940.0 cm^{-1} [Figure 1(*c*)]. These new bands were virtually coincident with those reported by Franzreb *et al.*[11] for $[Re(\eta^5\text{-}C_7H_7)(CO)_3]$ in hexane solution at 2 036, 1 966, and 1 943 cm^{-1}, leading to the assignment of the second photoproduct to the η^5 species (**3**). This moiety has resulted from two successive carbonyl ejections from the parent species (**1**) and an accompanying increase in ring hapticity. As before, a range of long-wavelength photolyses failed to produce any reversal in the form of a decrease in the intensities of any of the new bands due to the photoproducts.

Continued photolysis (filter A, total 120 min) resulted in further increases in the bands due to (**2**) and (**3**) at the expense of those of the parent complex (**1**) [Figure 1(*d*)]. A final period of photolysis (filter A, total 240 min) led to a complete disappearance of the i.r. bands due to the starting complex (**1**), the virtual disappearance of those assigned to the initial photoproduct (**2**), and a marked increase in those due to $[Re(\eta^5\text{-}C_7H_7)(CO)_3]$ (**3**) and 'free CO.' Two new bands were also found at 1 972.0 and 1 874.0 cm^{-1} under these extended-photolysis conditions due to a new photoproduct (**4**) (Table 1).

A series of subtractions conducted throughout the progress of the photolysis confirmed that the growth of the bands associated with each new photoproduct was accompanied by a decrease in the intensity of the bands due to the previous species and an increase in the band due to 'free CO.' Even in the case of the conversion (**3**) ⟶ (**4**) where the relative intensities of the bands and the coincident occurrence of the conversion (**2**) ⟶ (**3**) led to some problems, clear evidence of the interdependence of the photoproducts was still obtained in short periods of photolysis at times greater than 240 min. Very prolonged photolysis (>300 min) led to a decrease in the intensities of the bands due to both (**3**) and (**4**), *i.e.* photochemical decomposition became the major reaction pathway. Although a range of long-wavelength photolyses was performed at all stages during the various experiments, no reversal of the photoreactions was observed at any stage and the forward reactions were not significantly slower in a pure CO matrix than in Ar, although the reactions in CH_4 were faster.[17,18]

The only reasonable assignment for the initial photoproduct (**2**) is to the species $[Re(\eta^3\text{-}C_7H_7)(CO)_4]$ produced upon decarbonylation of the parent species and an accompanying increase in ring hapticity [see below, section (*iv*), comparison with manganese analogue]. The fact that four i.r. bands are observed for (**2**) implies that it has C_s symmetry rather than 'local C_{4v}' symmetry in the matrix environment. Identical symmetry arguments have been used in the case of other such species, specifically $[Mn(\eta^3\text{-}C_3H_5)(CO)_4]$,[19] confirming a C_s symmetry. Those authors were able to define the exact conformation and the location of the mirror plane using a combination of i.r. and Raman spectroscopy. The two new bands which appear at 1 972.0 and 1 874.0 cm^{-1} for the final photoproduct (**4**) and the fact that they arise from the decarbonylation of the η^5 species (**3**) leads to the assignment of the final species as $[Re(\eta^7\text{-}C_7H_7)(CO)_2]$. Experiments with the manganese analogue indicate that the $Re(CO)_2$ moiety has C_{2v} symmetry. No evidence was seen for any of the likely intermediates between the observed species, *i.e.* the 16-electron CO-loss products prior to 'ring slippage' such as $[Re(\sigma\text{-}C_7H_7)(CO)_4]$. This suggests that the actual 'ring slip' occurs fairly readily once CO ejection has taken place.

Photochemical studies of compound (**1**) by Graham[20] in nitrogen-purged solution using the ulfiltered arc of a medium-pressure mercury lamp produced a wide range of species but

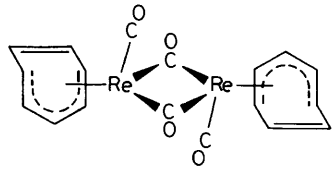

(**5**)

none with all seven ring carbon atoms bound to the Re metal centre. Extremely prolonged photolysis led mostly to decomposition with an unusual metal dimer being produced in very low yield (*ca.* 6%). The species $[\{Re(\eta^5\text{-}C_7H_7)(CO)_2\}_2]$ (**5**) was characterised by its n.m.r. spectra and *X*-ray crystal structure.

(*ii*) *Photolysis of* $[Re(\sigma\text{-}C_7H_7)(CO)_5]$ *isolated at High Dilution in Nitrogen and* ^{13}CO*-doped Methane Matrices at* ca. 12 K.—The intention of using such 'reactive matrices' as N_2 and

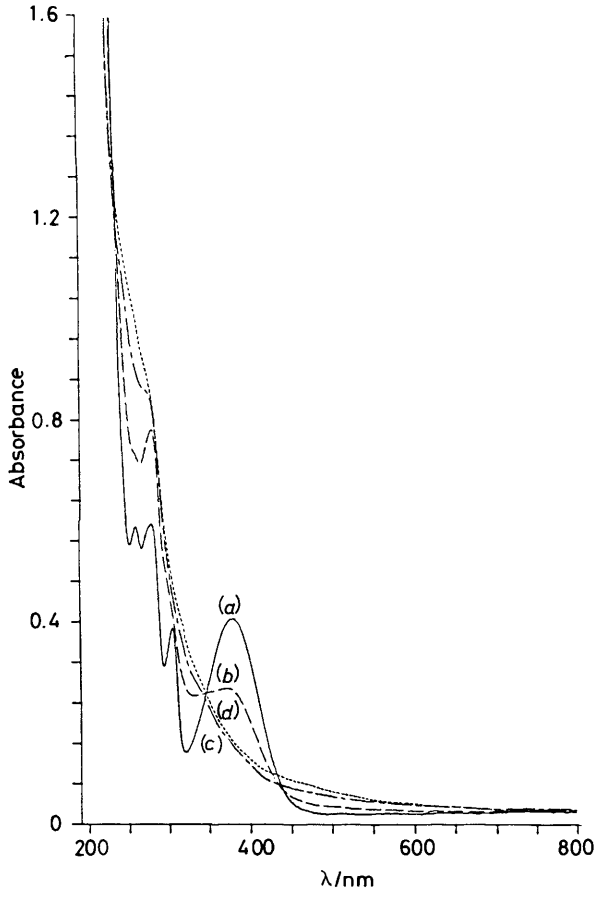

Figure 2. U.v.–visible spectra (Perkin-Elmer Lambda 7) of [Re(σ-C_7H_7)$(CO)_5$] and its photoproducts isolated at high dilution in an argon matrix at 12 K: (*a*) at start, (*b*) 20 min, (*c*) 120 min, and (*d*) 240 min with filter A

^{13}CO-doped CH_4 was to enable the 'reactive doped species' to be incorporated into the photoproducts or parent molecule in one of two ways. First, if a photoinduced back reaction occurs then the photoproduct may pick up a labelled ligand rather than the originally photoejected ligand, *e.g.* CO. Secondly, incorporation of a labelled ligand may occur immediately after photoejection of a ligand during the 'cage recombination' stage due to a competition between the ejected ligand and a labelled ligand in close proximity with or as part of the cage.

Since no 'back reaction' could be photoinduced for any of the species (**2**)—(**4**) useful information was only likely to be obtained if the second set of conditions above applied. This was not the case and analogous results to those seen in Ar, CH_4, and CO matrices were observed with, again, slight band shifts due to differences in the microscopic matrix environment.

(*iii*) *U.v.–Visible Spectra of Species formed on the Photolysis of* [Re(σ-C_7H_7)$(CO)_5$] *isolated at High Dilution in* Ar, CH_4, CO, *and* N_2 *Matrices at* ca. 12 K.—The u.v.–visible spectrum of compound (**1**) isolated at high dilution in an argon matrix is shown in Figure 2(*a*). The spectrum agrees well with that seen in hexane solution solution except that the shoulder previously at *ca.* 305 nm has become a band at 304 nm due to the increased resolution in low-temperature matrix.

In order to relate changes in the u.v.–visible spectra to the species formed during photolysis, matrix experiments were followed simultaneously by both i.r. and u.v.–visible spectroscopy. The u.v.–visible spectra presented in Figure 2 relate directly to the i.r. spectra shown in Figure 1.

Initial photolysis (filter A, total 20 min) led to the appearance of species (**2**), which from the changes in the u.v.–visible spectrum [Figure 2(*b*)] has a sharp absorption at 280 nm. Continued photolysis (filter A, total 120 min) resulted in a mixture of (**2**) and (**3**) and led to an increase in the absorbance in the 260—280 nm region as well as the disappearance of all the absorptions associated with the parent species [Figure 2(*c*)]. I.r. evidence also showed very little (**1**) present at this stage [Figure 1(*d*)]. Further photolysis (filter A, total 240 min) resulted chiefly in species (**3**) with a very small amount of (**4**) [Figure 1(*e*)]. Hence, the u.v.–visible spectrum at this stage was largely due to species (**3**) and it can be concluded that this species shows an absorption at *ca.* 270 nm which appears in the overall spectrum as a shoulder [Figure 2(*d*)]. This is in reasonable agreement with the bands reported for the analogue [Mn(η^5-C_7H_7)$(CO)_3$] by Budnik and Whitesides;[5] (ethanol) 262 nm (ε = 10 400) and 307 nm (shoulder, ε = 4 500) although the shoulder at 307 nm was not resolved.

(*iv*) *Photolysis of* [Mn(C_7H_7CO)$(CO)_5$] *isolated at High Dilution in* Ar, CH_4, *and* CO *Matrices at* ca. 12 K.—The i.r. spectrum of [Mn(C_7H_7CO)$(CO)_5$] (**6**) isolated at high dilution in a methane matrix is shown in Figure 3(*a*). The spectrum indicates that the $Mn(CO)_5$ fragment has local C_s symmetry, all five terminal CO stretches being i.r. active with bands at 2 118.0, 2 053.5, 2 021.5, 2 010.5, and 2 002.5 cm^{-1} with the acyl stretch at 1 656.0 cm^{-1}. Budnik and Whitesides[5] report only three terminal CO stretching vibrations for (**6**) in pentane solution at 2 115, 2 050, and 2 005 cm^{-1} with the acyl stretch at 1 652 cm^{-1}. The contrast between the solution spectrum and that seen in matrices and the difference between the matrix spectra of compound (**1**) and (**6**) must be due to the presence of the acyl moiety. Ideally the acyl group would be freely rotating, whilst on deposition in a matrix it will be 'trapped out' in one or more probably in a number of low-symmetry conformations. In solution the acyl group is much less constrained being free to adopt the most favoured and in this case clearly more symmetric conformer although of course bond rotation will still occur. The same is true for comparisons with (**1**) for which it appears the quasi-axial configuration appears to predominate in all phases.

The solution (n-hexane) u.v.–visible spectrum of (**6**) was rather featureless showing one very strong and two weak absorptions; 214 (ε = 33 000), 295 (shoulder, ε = *ca.* 5 300), and 360 nm (shoulder, ε = *ca.* 800 dm^3 mol^{-1} cm^{-1}). Initial brief photolysis (filter B, total 5 min) at 290 < λ < 370 >550 nm, led to a decrease in the intensity of the i.r. bands attributed to (**6**) and the appearance of a band due to 'free CO' at 2 136.3 cm^{-1} as well as a number of new bands [Figure 3(*b*)]. The new bands at 2 086.5, 1 994.0, and 1 951.0 cm^{-1} [one band obscured by that of (**8**) at 1 991.0 cm^{-1}] can be associated with [Mn(C_7H_7CO)$(CO)_4$] (**7**) by comparison with the bands for [Mn(MeCO)$(CO)_4$] in low temperature matrices.[18] The ketonic band of this species was too weak to be observable even in a subtraction spectrum due to problems with matrix-isolated water and background absorptions due to atmospheric water vapour. Other new bands at 2 112.5, 2 015.0, and 1 991.0 cm^{-1} demonstrate the presence of [Mn(σ-C_7H_7)$(CO)_5$] (**8**) by analogy with the band positions of [Mn$(CO)_5$Me] in low-temperature matrices[18] and also with those of (**1**). A range of long-wavelength photolyses failed to produce any photochemical reversal, although moderate photolysis (filter C, 10 min) at 380 < λ 440 led to photoconversion of (**7**) into (**8**).

Continued photolysis (filter B, total 15 min) resulted in the continued decrease in bands due to (**6**) and increases in those of (**8**) and 'free CO' [Figure 3(*c*)]. The intensities of the bands assigned to compound (**7**) remained approximately constant. New bands appeared at 2 067.5, 1 984.0, 1 962.0, and 1 957.0 cm^{-1} which can be assigned to [Mn(η^3-C_7H_7)$(CO)_4$] (**9**) by

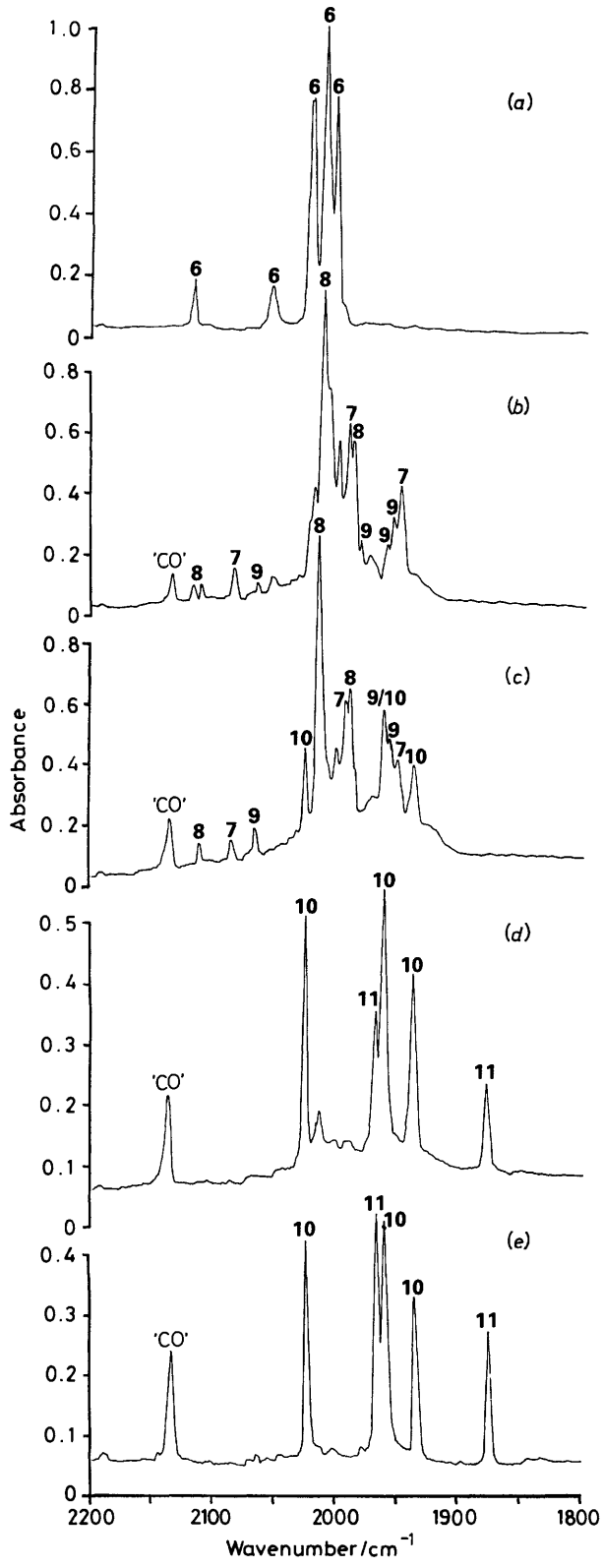

Figure 3. Infrared spectra (Nicolet 7199) (CO-stretching region) of $[Mn(C_7H_7CO)(CO)_5]$ and its photoproducts isolated at high dilution in a methane matrix: (*a*) at start, (*b*) 5 min, (*c*) 15 min, (*d*) 45 min, and (*e*) 90 min with filter B

comparison with the bands due to $[Mn(\eta^3\text{-}C_3H_5)(CO)_4]$ at 2 068, 1 989, 1 974, and 1 958 cm^{-1} in CS_2 solution. Additional new bands also appeared at 2 026.1, 1 962.5, and 1 938.5 cm^{-1}.

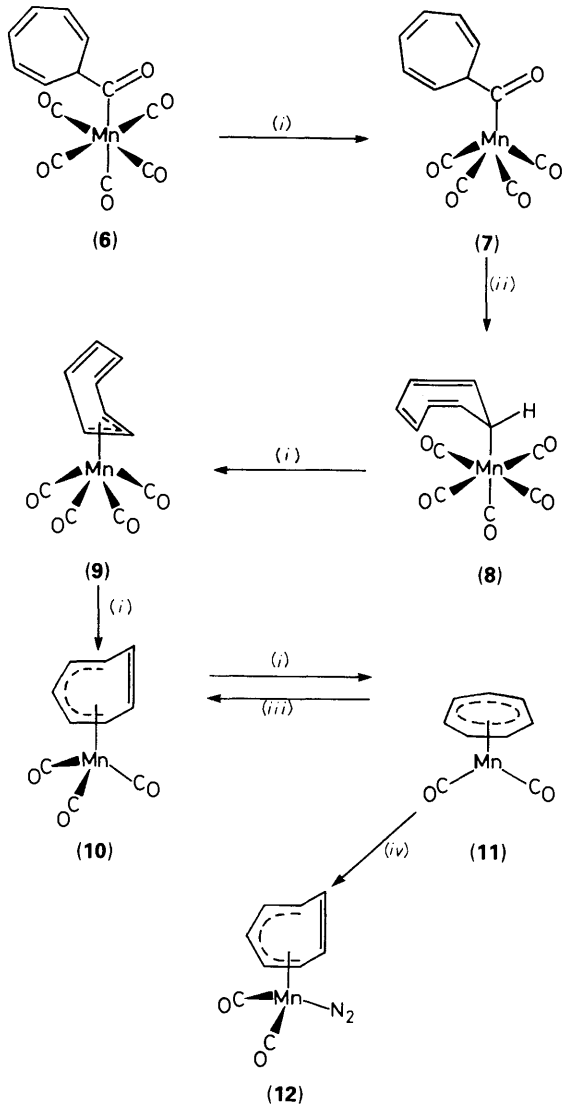

Scheme 3. The photoreactions of $[Mn(C_7H_7CO)(CO)_5]$ isolated at high dilution in various matrices at 12 K. (*i*) *hν*, −CO, filter B; (*ii*) *hν'*, filter C; (*iii*) *hν''*, +CO, filter D; (*iv*) *hν''*, $+N_2$, filter D

These can be assigned to $[Mn(\eta^5\text{-}C_7H_7)(CO)_3]$ (**10**) by comparison with the band positions reported for this species in CS_2 solution by Budnik and Whitesides.[5] Again a range of long-wavelength photolyses failed to produce reversal of any of the photoproducts present at this stage.

Further photolysis (filter B, total 45 min) resulted in the disappearance of all bands associated with the species (**6**)—(**8**) and the virtual disappearance of those assigned to (**9**). The band due to 'free CO' increased markedly as did the bands of (**10**) [Figure 2(*d*)]. Two further bands were observed at 1 969.0 and 1 879.0 cm^{-1} (Table 2).

A final period of photolysis (filter B, total 90 min) resulted in a marked increase in the two new bands. A substraction showed that the growth of these bands was clearly associated with a decrease in the intensity of the bands of (**10**) and an increase in the band due to 'free CO.' On this basis and by comparison with species (**4**) the new bands were assigned to the dicarbonyl species $[Mn(\eta^7\text{-}C_7H_7)(CO)_2]$ (**11**) (see also Discussion). Unlike at all previous stages, a short period of long-wavelength photolysis (filter D, total 10 min) at $\lambda > 460$ nm led to photochemically induced reversal of (**11**) to (**10**) with an accompanying decrease in the intensity of the band due to 'free

Table 2. Infrared band positions (cm^{-1})[a] for $[Mn(C_7H_7)(CO)_5]$ and the terminal and ketonic CO-stretching region and its photoproducts in argon, methane, and carbon monoxide matrices

Complex	ν_{CO}	Ar	CH_4	CO
(6) $[Mn(C_7H_7CO)(CO)_5]$	A'	2 120.0w	2 118.0w	2 112.5w
C_s	A'	2 056.0w	2 053.5w	2 056.5w
	A'	2 024.5s	2 021.5s	2 022.0s
	A''[b]	2 013.0vs	2 010.5s	2 013.5s
	A'	2 006.5m	2 002.5s	2 005.0s
	A'	1 661.0w	1 656.0w	1 648.5w
(7) $[Mn(C_7H_7CO)(CO)_4]$	A'	2 089.0w	2 086.5w	*c*
C_s	A'	2 005.5s	1 994.0s	1 995.0s
	A''	*d*	*d*	*d*
	A'	1 955.5m	1 951.0m	1 952.5m
	A'	*e*	*e*	*e*
(8) $[Mn(\sigma\text{-}C_7H_7)(CO)_5]$	A_1	2 114.0w	2 112.5w	*f*
C_{4v}	E	2 016.5vs	2 015.0vs	2 015.0vs
	A_1	1 995.5m	1 991.0m	1 994.0m
(9) $[Mn(\eta^3\text{-}C_7H_7)(CO)_4]$	A'	2 069.0w	2 067.5w	2 067.5w
C_s	A'	1 987.5w	1 984.0w	1 984.0w
	A''	1 973.5m	1 962.0m	1 972.0m
	A'	1 962.0m	1 957.0m	1 965.5s
(10) $[Mn(\eta^5\text{-}C_7H_7)(CO)_3]$	A'	2 028.5vs	2 026.1s	2 027.0s
C_s	A''	1 965.0s	1 962.5s	1 963.5vs
	A'	1 943.0m	1 938.5m	1 937.5m
		1 941.5m		
(11) $[Mn(\eta^7\text{-}C_7H_7)(CO)_2]$	A_1	1 971.5m	1 969.0m	1 971.5m
C_{2v}	B_1	1 881.5m	1 879.0m	1 878.0m

[a] Bands bracketed together arise from a single fundamental with matrix splitting. [b] These three bands form an overlapped multiplet. [c] Band obscured by the matrix band of ^{13}CO. [d] Band obscured by the low-wavenumber A_1 band of compound (**7**). [e] Band obscured by the matrix-isolated H_2O band and by problems due to atmospheric water vapour in this region. [f] Band obscured by the matrix band of $C^{18}O$.

Table 3. Infrared band positions (cm^{-1}) for $[Mn(C_7H_7CO)(CO)_5]$ in the terminal and ketonic CO-stretching region and its photoproducts in pure nitrogen matrices

Complex	ν_{CO}	N_2
(6) $[Mn(C_7H_7CO)(CO)_5]$	A'	2 121.0w
	A'	2 057.5w
	A'	2 024.0s
	A''[b]	2 014.5vs
	A'	2 008.0m
		2 006.0m
	A'	1 659.0vw
(7) $[Mn(C_7H_7CO)(CO)_4]$	A'	2 087.5w
	A'	2 002.5s
	A''	*c*
	A'	1 952.0m
	A'	*d*
(8) $[Mn(\sigma\text{-}C_7H_7)(CO)_5]$	A_1	2 114.5w
	E	2 017.5vs
	A_1	1 997.0m
(9) $[Mn(\eta^3\text{-}C_7H_7)(CO)_4]$	A'	2 069.0w
	A'	1 985.5w
	A''	1 973.0m
	A'	1 966.0s
(10) $[Mn(\eta^5\text{-}C_7H_7)(CO)_3]$	A'	2 030.0s
	A''	1 970.0m
		1 966.5s
	A'	1 942.5w
(12) $[Mn(\eta^5\text{-}C_7H_7)(CO)_2(N_2)]$[e]	A'	1 981.5
	A''	1 927.0
(11) $[Mn(\eta^7\text{-}C_7H_7)(CO)_2]$	A_1	1 973.0s
	B_1	1 882.0m

[a] Bands bracketed together arise from a single fundamental with matrix splitting. [b] These three bands form an overlapped multiplet. [c] Band obscured by the low-wavenumber A_1 band of compound (**8**). [d] Band obscured by the matrix-isolated H_2O band and by problems due to atmospheric water vapour in this region. [e] ν_{NN} at 2 163.5 cm^{-1}. Bands were too weak to establish their relative intensities.

CO.' Reversal was enhanced in a pure CO matrix, but only to a moderate extent.

(*v*) *Photolysis of* $[Mn(C_7H_7CO)(CO)_5]$ *isolated at High Dilution in Nitrogen and* ^{13}CO*-doped Methane Matrices at* ca. 12 K.—Photolysis of compound (**6**) led to identical photochemistry to that seen in other matrices, with small differences in band positions due to differing matrix-solvent effects and packing (Table 3). However, an additional reaction occurred once 90 min of photolysis had produced approximately equal quantities of species (**10**) and (**11**) [an equivalent situation to that shown in Figure 3(*e*)]. In this situation 29 min of photolysis with filter D resulted not only in the 'back reaction' producing (**10**) from (**11**) and 'free CO' but also in the appearance of three new weak i.r. bands. These bands in the terminal CO-stretching region at 1 981.5 and 1 927 and at 2 163.5 cm^{-1} in the region expected for the nitrogen–nitrogen stretch of a dinitrogen ligand can be assigned to the dinitrogen substitution product $[Mn(\eta^5\text{-}C_7H_7)(CO)_2(N_2)]$ (**12**). The band positions observed for this complex agreed well with those reported for the analogous cyclopentadienyl complex $[Mn(\eta^5\text{-}C_5H_5)(CO)_2(N_2)]$ by Sellmann[21] at 2 169, 1 980, and 1 923 cm^{-1} in n-hexane. It is clear that species (**12**) was produced when a photoexcited molecule of (**11**) recombined with a nitrogen molecule of the matrix cage, rather than with one of the originally photoejected CO ligands. The fact that CO recombination also occurs indicates that the two processes are in competition. Further periods of forward photolysis (filter B) followed by attempted reversal (filter D) failed to produce any new i.r. bands which would have been expected either for the N_2 analogue of (**11**) $[Mn(\eta^7\text{-}C_7H_7)(CO)(N_2)]$ or the bis-(dinitrogen) analogue of (**10**) $[Mn(\eta^5\text{-}C_7H_7)(CO)(N_2)_2]$. The absence of these species indicated that photolysis of (**12**) either resulted predominantly in loss of N_2 regenerating (**11**) or more probably that any such species were formed in such low yield [given that the amount of (**12**) formed was small anyway] that their i.r. bands were undetectable above the 'baseline noise' even in extremely expanded subtractions.

Photolysis of compound (**6**) in a 5% ^{13}CO-doped methane matrix again followed the familiar pattern, 75 min of photolysis with filter B producing an approximately equal quantity of species (**10**) and (**11**). In order to calculate an energy-factored force field for the two species the band positions of all possible ^{13}CO-substitution products were required. To achieve this repeated periods of forward photolysis were interspersed with periods of photoreversal in order to generate a 'scrambling effect.' This repeated photolysis took the form of six periods of 15 min with filter B plus 15 min of filter D. Eventually, all the necessary species were generated, although the bands due to the tris-^{13}CO-substituted (**10**) and the bis-^{13}CO-substituted (**11**) were very weak and only showed on a vastly expanded scale, whilst some bands were obscured by stronger bands due to other species. The full range of band positions for the substituted species is shown in Table 4. The calculated bands shown are for the best fit obtained by comparison with the observed bands. In the case of (**10**) this involved a C_s $Mn(CO)_3$ fragment with one unique and two equivalent carbonyls. For (**11**) the best fit was obtained for a C_{2v} $Mn(CO)_2$ fragment. The agreement between the observed and calculated band positions was good and served to confirm the assignments of species (**10**) and (**11**) and by analogy (**3**) and (**4**).

Table 4. Observed (Nicolet 7199) and calculated[a] wavenumbers (cm^{-1}) of terminal i.r. CO-stretching bands produced following photolysis of $[Mn(C_7H_7CO)(CO)_5]$ in a 5% ^{13}CO-doped methane matrix at 12 K

Complex	ν_{CO}	Observed	Calculated
$[Mn(\eta^5\text{-}C_7H_7)(^{12}CO)_3]$	A'	2 025.5	2 024.7
C_s	A'	1 961.0	1 961.5
	A''	1 937.0	1 937.5
$[Mn(\eta^5\text{-}C_7H_7)(^{12}CO)_2(^{13}CO)]$	A'	2 014.5[c]	2 015.0
C_s isomer 1[b]	A''	*d*	1 937.6
	A'	*e*	1 927.1
C_1 isomer 2[f]	A	2 014.5[c]	2 014.2
	A	*d*	1 957.6
	A	1 907.0[g]	1 908.3
$[Mn(\eta^5\text{-}C_7H_7)(^{12}CO)(^{13}CO)_2]$	A'	2 000.5	2 000.8
C_s isomer 3[h]	A'	*e*	1 928.8
	A''	1 907.0[g]	1 906.2
C_1 isomer 4[i]	A	2 002.5	2 002.5
	A	*d*	1 939.1
	A	*j*	1 895.0
$[Mn(\eta^5\text{-}C_7H_7)(^{13}CO)_3]$	A'	1 979.0	1 979.7
	A'	1 918.5	1 917.9
	A''	1 895.0	1 894.5
$[Mn(\eta^7\text{-}C_7H_7)(^{12}CO)_2]$	A_1	1 965.5	1 965.4
	B_1	1 877.5	1 876.7
$[Mn(\eta^7\text{-}C_7H_7)(^{12}CO)(^{13}CO)]$	A'	1 948.0	1 948.4
	A''	1 850.5	1 951.0
$[Mn(\eta^7\text{-}C_7H_7)(^{13}CO)_2]$	A_1	*j*	1 921.7
	B_1	1 834.5	1 835.0

[a] Refined energy-factored force constants for $[Mn(\eta^5\text{-}C_7H_7)(CO)_3]$: K_1 = 1 588.3, K_2 = 1 569.5, k_{12} = 33.9, and k_{23} = 52.8 N m^{-1} as defined by the numbering shown below, *i.e.* 1 ≠ 2 = 3. Refined energy-

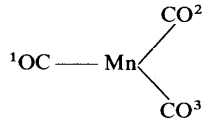

factored force constants for $[Mn(\eta^7\text{-}C_7H_7)(CO)_2]$: K = 1 491.8 and k_i = 68.8 N m^{-1}. Calculations based on the method and program already described (D. J. Taylor, Ph.D. Thesis, University of Southampton, 1981). [b] ^{13}CO in position 1. [c] Component of broad band. [d] Band obscured by bands of $[Mn(\eta^5\text{-}C_7H_7)(^{12}CO)_3]$. [e] Component on the shoulder of a band of $[Mn(\eta^5\text{-}C_7H_7)(^{12}CO)_3]$. [f] ^{13}CO in position 2. [g] Component of a broad band centred at 1 907 cm^{-1}. [h] ^{12}CO in position 1. [i] ^{12}CO in position 2. [j] Band obscured by bands of ^{13}CO-enriched $[Mn(\eta^5\text{-}C_7H_7)(CO)_3]$.

(*vi*) *U.v.–Visible Spectra of Species formed on Photolysis of* $[Mn(C_7H_7CO)(CO)_5]$ *at High Dilution in* Ar, CH_4, CO, *and* N_2 *Matrices at* ca. 12 K.—The u.v.–visible spectrum of compound (**6**) isolated at high dilution in a methane matrix is shown in Figure 4(*a*). The absorption seen at 214 nm in hexane solution is obscured by scattering effects in the matrix, but the longer-wavelength shoulder and the weak absorption seen in solution are observed at 290 and 360 nm respectively in the matrix.

Initial photolysis (filter B, total 15 min) leading to a situation where the major species present was (**8**) resulted in the appearance of a shoulder at *ca.* 280 nm and a weak absorption at *ca.* 410 nm [Figure 4(*b*)] in reasonable agreement with the spectrum seen for the rhenium analogue (**1**) [Figure 2(*a*)].

Further photolysis (filter B, total 30 min) led to a situation where the predominant species present according to i.r. spectroscopy was (**10**) which resulted in the appearance of a shoulder at 302 nm and weaker absorptions at 380 and 490 nm [Figure 4(*c*)]. The shoulder was reported by Budnik and Whitesides at 307 nm in ethanol,[5] but the weaker bands were presumably too weak to be resolved at room temperature. The band at 262 nm reported for this species by the same authors was too intense to be observed under matrix conditions designed to monitor u.v.–visible and i.r. spectra from the same sample.

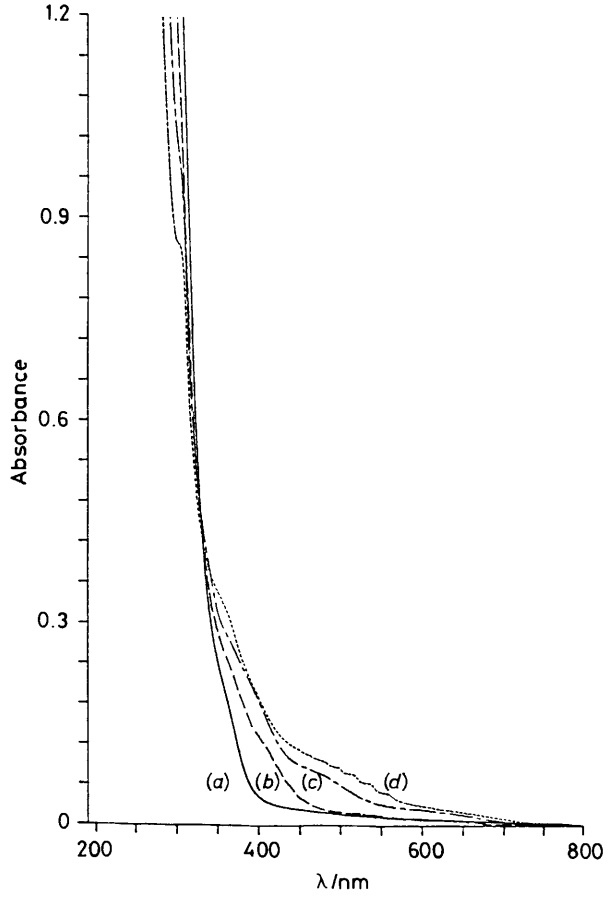

Figure 4. The u.v.–visible spectra (Perkin-Elmer Lamdba 7) of $[Mn(C_7H_7CO)(CO)_5]$ and its photoproducts isolated at high dilution in a methane matrix at 12 K: (*a*) at start, (*b*) 15 min, (*c*) 30 min, and (*d*) 90 min with filter B

A final period of photolysis (filter B, total 90 min) resulted in the production of an almost equal quantity of species (**10**) and (**11**), *i.e.* an identical situation to that seen in Figure 3(*e*). In the absorption spectrum the shoulder at 320 nm due to (**11**) became well resolved and two new absorption bands due to (**11**) appeared at 365 and *ca.* 525 nm, the latter showing pronounced vibrational structure [Figure 4(*d*)]. An expansion of the 450—600 nm region and the computation of the second derivative of the spectrum (Figure 5) enabled the vibrational splitting of the peak at *ca.* 525 nm to be calculated as 738 ± 14 cm^{-1}. This prompted a re-examination of the i.r. spectra for (**1**), (**6**), and their photoproducts in the low-wavenumber (1 200—300 cm^{-1}) region.

The shoulder observed at 302 nm for compound (**10**) is shown to have an absorption coefficient of *ca.* 4 500 dm^3 mol^{-1} cm^{-1} in solution[5] and this allowed a very approximate calculation of the band intensities of the weak bands of (**10**) and (**11**) to be made. From such a comparison the bands were assigned the following intensities: (**10**), 389 (ε = *ca.* 1 000) and 480 (ε = *ca.* 400); (**11**), 365 (ε = *ca.* 1 500) and 525 nm (ε = *ca.* 400 dm^3 mol^{-1} cm^{-1}).

The u.v.–visible spectra obtained upon photolysis of (**6**) in a pure nitrogen matrix were identical to those in the other three matrices, no new bands being seen for species (**12**), although this was undoubtedly due to the low yield in which it was formed.

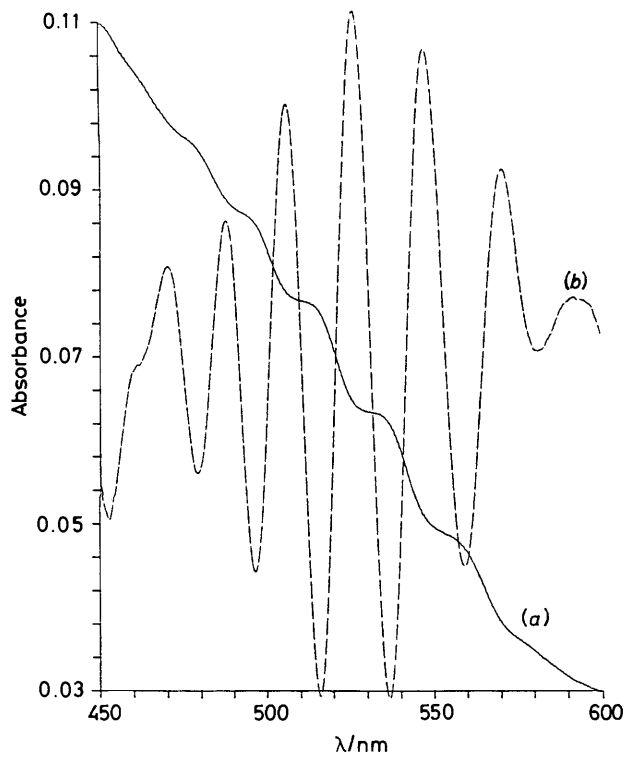

Figure 5. The u.v.–visible spectrum (Perkin-Elmer Lamdba 7) of $[Mn(C_7H_7)(CO)_2]$ (**11**) isolated at high dilution in a methane matrix at 12 K showing the vibrational structure in the 450—600 nm region: (*a*) absorption spectrum and (*b*) second derivative

Table 5. Infrared band positions (cm^{-1})[a] for $[Re(\sigma\text{-}C_7H_7)(CO)_5]$, $[Mn(C_7H_7CO)(CO)_5]$, and their photoproducts in the CO and C_7H_7 deformation regions in argon, methane, and carbon monoxide matrices

Complex	Ar	CH_4	CO	Assignment
(**1**) $[Re(\sigma\text{-}C_7H_7)(CO)_5]$	721m	717m	715m	C–C str[b]
	606s	602s	603s	C–O def
	592m	590m	590m	C–O def
(**3**) $[Re(\eta^5\text{-}C_7H_7)(CO)_3]$	727w	725w	725w	C–C str[b]
	610w	612w	608w	C–O def
	605s	604s	605s	C–O def
	592m	590m	590m	C–O def
(**6**) $[Mn(C_7H_7CO)(CO)_5]$	770m	770w, 764m	768m	C–C str[b]
	672m	670m	672m	C–O def
	665w	662vw	661vw	C–O def
	658s	657vs	656s	C–O def
	652s	651s	651s	C–O def
(**10**) $[Mn(\eta^5\text{-}C_7H_7)(CO)_3]$	712m	712m	710m	C–C str[b]
	668s	664s	662s	C–O def
	660s	658vs	654s	C–O def
	643m	642m	640m	C–O def
(**11**) $[Mn(\eta^7\text{-}C_7H_7)(CO)_2]$	737m	734m	733m	C–C str[b]
	610m	607m	607m	C–O def
	598vw	598vw	597vw	C–O def

[a] Bands bracketed together arise from a single fundamental with matrix splitting. [b] Tentative assignment.

(*vii*) *Infrared Spectra in the Low-wavenumber region* (1 200—300 cm^{-1}) *for Experiments involving Photolyses of* $[Re(\sigma\text{-}C_7H_7)(CO)_5]$ *and* $[Mn(C_7H_7CO)(CO)_5]$ *isolated at High Dilution in* Ar, CH_4, CO, *and* N_2 *Matrices at* ca. 12 K.—The i.r. spectrum of $[Mn(C_7H_7CO)(CO)_5]$ (**6**) isolated at high dilution in a methane matrix is shown in Figure 6(*a*) between 800 and 600 cm^{-1}, the region that proved to be of primary interest.

The band assignments given are all tentative since there are discrepancies in the literature over the precise nature of the vibrations of these species in this region. The assignments were based upon the band positions for the 'free tropylium cation' given by Graham and Howard,[22] the bands for $[V(\eta^7\text{-}C_7H_7)(CO)_3]$ reported by Manastyrskyj and Werner[6] and assigned by Fritz,[23] and the band positions of $[M(\eta^7\text{-}C_7H_7)(CO)_3]^+$ species (M = Cr, Mo, or W) reported by Graham and Howard[22] and Butler *et al.*[24] Four bands were observed for (**6**) in the CO deformation region [Figure 6(*a*)] at 670, 662, 657, and 651 cm^{-1} and two bands or possibly one band which was matrix split in the ring-deformation region at 770 and 764 cm^{-1} (Table 5).

The next clearly assignable bands were for species (**10**) and these were observed following 60 min of photolysis with filter B. The CO deformations for (**10**) appeared at 664, 658, and 642 cm^{-1} whilst one 'ring mode' was observed at 712 cm^{-1}.

Further photolysis (filter B, total 120 min)* resulted in the appearance of bands due to (**11**) which showed two CO deformations at 607 and 598 and a 'ring mode' at 734 cm^{-1} [Figure 6(*c*)]. This mode was in excellent agreement with the vibrational structure seen on the band at *ca.* 525 nm attributed to (**11**) in the u.v.–visible spectrum.

Similar experiments were performed using $[Re(\sigma\text{-}C_7H_7)(CO)_5]$ and these yielded clearly assignable band positions for species (**1**) and (**3**) which are also shown in Table 5.

From a comparison of the studies mentioned above the actual nature of the 'ring mode' was not immediately clear. For the cationic species of Cr, Mo, and W both Graham and Howard[22] and Butler *et al.*[24] quote a band position of *ca.* 860 cm^{-1} for the A_1 stretching mode of the ring carbon skeleton. This initially appeared to be at too high a frequency. However, a comparison of the C–O stretching modes for the cations as against the neutral species of Mn and Re also shows a frequency shift of *ca.* 100 cm^{-1}, which can be attributed to an increase in metal-to-ligand π 'backbonding' for the neutral species. This was entirely consistent with the cationic species possessing a relatively electron-poor metal centre. Hence such a large shift in the 'ring mode' for the neutral species was not as at first appeared anomalous. Such an assignment was also supported by the fact that for (**11**) the vibrational structure seen on the band at *ca.* 525 nm implied some metal-to-ligand charge-transfer character to the transition and so a mode which involved the distortion of the ring carbon skeleton seemed far more reasonable than for example a C–H deformation.

Discussion

The photoreactions of $[Re(\sigma\text{-}C_7H_7)(CO)_5]$ and $[Mn(C_7H_7CO)(CO)_5]$ isolated at high dilution in a variety of matrices are summarised in Schemes 2 and 3 respectively. Both species show the same general behaviour, with differences in specific details. This was only to be expected given the differing natures of the general chemistry of Mn and Re and more specifically the differing photochemical behaviour of the $[M(C_7H_7CO)(CO)_5]$ (M = Mn or Re) moiety in low-temperature solution which had in fact initiated the study.[4,5]

Once the acyl CO extrusion reaction had occurred for (**7**) forming the σ species (**8**) the chemistry of both the manganese and the rhenium species followed the same pattern of CO loss accompanied by a change in ring hapticity. The fact that no 16-

* Photolysis times were longer than in previous experiments because KBr and CsI rather than CaF_2 spectroscopic windows were used for this region.

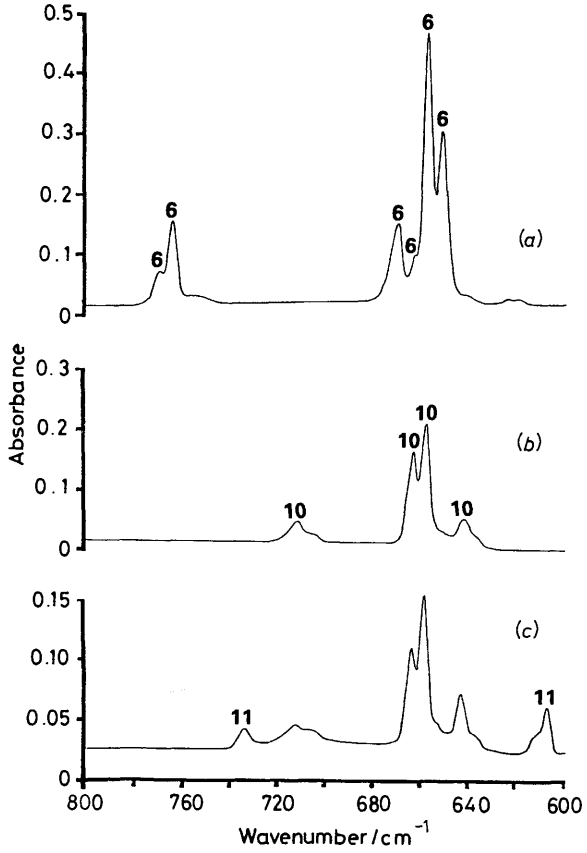

Figure 6. Infrared spectra (Perkin-Elmer 983G) (800—600 cm^{-1} region) of $[Mn(C_7H_7CO)(CO)_5]$ and its photoproducts isolated at high dilution in a methane matrix: (*a*) at start, (*b*) 60 min, and (*c*) 120 min with filter B

electron CO-loss species were observed prior to 'ring slippage' even given the low temperatures involved indicated that either such 'ring slips' occur extremely readily or they occur as a concerted process along with CO loss. In either case the implication is that such processes, although as yet only implied in room-temperature solution studies, have potentially great mechanistic importance in the chemistry of such metal–arene species.

The use of a higher-energy photolysis source for Re over Mn was expected from the low-temperature solution studies which had demonstrated the greater stability of the rhenium species. The fact that, even given the higher-energy photolysis source used in the case of the latter far longer photolysis times had to be used to produce the same photochemistry as for the manganese species can be explained on the grounds of an increased 'internal heavy-atom effect' for Re. This effect involving the greater spin–orbit coupling of the Re metal centre resulted in an increase in the efficiency of non-radiative pathways for Re over Mn. The net effect of such a process was to depopulate the excited state in the case of Re, resulting in a lower quantum yield of photochemical reaction for the series of rhenium species as compared to their manganese analogues.

Such arguments can also be used to account for the lower yield of the rhenium η^7 species (**4**) over its manganese analogue (**11**), with prolonged photolysis in the case of the rhenium experiments resulting in photochemical decomposition of all the species present. The lack of photochemically induced reversibility in the case of (**4**) may be attributed to two causes. First, the increased metal–ligand bond strength for Re as against Mn and secondly the increased size of the Re metal centre which may be able to accommodate the C_7H_7 ring much more readily than the smaller Mn metal centre.

The appearance of vibrational structure on the absorption band at *ca.* 525 nm of (**11**) indicated a high symmetry for this species, correlating well with the energy-factored force-field fitting study, which gave the best fit for (**11**) as a local C_{2v} symmetry rather than some lower symmetry structure. The fact that this band showed a vibrational progression which was attributable to a 'ring mode' implies that the absorption has significant metal-to-ligand charge-transfer character. This agrees well with the observation that it is photolysis into this band using filter D, $\lambda > 460$ nm, which produced (**11**) ⟶ (**10**) reversal. This implies that the excited state leading to reversal, *i.e.* CO addition, involves significant localisation on the η^7-C_7H_7 ligand, again highlighting the importance of such 'ring slip' processes in the mechanism of additions to metal–arene species.

In the i.r. spectrum the shift of the 'ring mode' from 710 to 733 cm^{-1} in CO matrices upon becoming planar, *i.e.* η^5-C_7H_7 ⟶ η^7-C_7H_7 in the conversion of (**10**) into (**11**) agrees well with the shift in band positions observed by Crichton *et al.* for the conversion of $[Co(\eta^3\text{-}C_5H_5)(CO)_3]$ into $[Co(\eta^5\text{-}C_5H_5)(CO)_2]$ of 780.9 to 817.3 cm^{-1} also in a CO matrix.[25] Such large shifts upon becoming planar support the assignment of the 'ring mode' to a 'ring breathing mode' rather than to a C–H wagging mode for which more modest shifts might be expected.

Conclusion

This study has demonstrated both the general similarities in the photochemistry of the two species under investigation and the specific differences, which have been explained on the basis of the differing natures of the two metal centres.

The ease with which 'ring slippage' was seen to occur demonstrates the potential mechanistic importance of such processes and highlights the relative dearth of information on this subject, chiefly due to the difficulty of studying such systems in room-temperature solutions.[8]

Acknowledgements

We thank Professors W. A. G. Graham and P. Hofmann for helpful discussions and for their generous gifts of compounds. We also thank the S.E.R.C. for a Studentship (to A. K. C.), for a Fellowship (to R. N.), and for support (to A. J. R).

References

1 M. J. Bennett, F. A. Cotton, A. Davison, J. W. Faller, S. J. Lippard, and S. M. Morehouse, *J. Am. Chem. Soc.*, 1966, **88**, 4371.
2 B. Dickens and W. N. Lipscomb, *J. Am. Chem. Soc.*, 1961, **83**, 4052; *J. Chem. Phys.*, 1962, **37**, 2084.
3 R. B. King and M. B. Bisnette, *Inorg. Chem.*, 1964, **3**, 785.
4 D. M. Heinekey and W. A. G. Graham, *J. Am. Chem. Soc.*, 1979, **101**, 6115; *J. Organomet. Chem.*, 1982, **232**, 335.
5 R. A. Budnik and T. H. Whitesides, *Chem. Commun.*, 1971, 1514; *Inorg. Chem.*, 1976, **15**, 874.
6 S. A. Manastyrskyj and R. R. M. Werner, *J. Am. Chem. Soc.*, 1961, **83**, 2023.
7 D. A. Brown, N. J. Fitzpatrick, M. A. McGinn, and T. H. Taylor, *Organometallics*, 1986, **5**, 152.
8 C. P. Casey and J. M. O'Connor, *Chem. Rev.*, 1987, **87**, 307.
9 F. Basolo, *Inorg. Chim. Acta*, 1985, **100**, 33.
10 F. A. Cotton and G. Wilkinson, 'Advanced Inorganic Chemistry,' 5th edn., Wiley, London, 1988, pp. 1331 and 1332.
11 K. H. Franzreb, C. G. Kreiter, and W. Michels, *Z. Naturforsch., Teil B*, 1985 **40**, 1188.
12 L. S. Brown, J. H. Connor, and H. A. Skinner, *J. Organomet. Chem.*, 1974, **81**, 403.
13 J. A. Connor, in 'Thermochemistry and its Applications to Chemical and Biochemical Systems,' NATO Advanced Studies Institutes Series C, ed. M. A. V. Ribeiro da Silva, Reidel, Dordrecht, 1984, p. 383.

14 R. B. Hitam, R. Narayanaswamy, and A. J. Rest, *J. Chem. Soc., Dalton Trans.*, 1983, 1351.
15 A. J. Barnes, in 'Vibrational Spectroscopy of Trapped Species,' ed. H. A. Hallam, Wiley, London, 1973, p. 133.
16 A. J. Barnes, in 'Matrix Isolation Spectroscopy,' NATO Advanced Studies Institutes Series C, eds. A. J. Barnes, W. J. Orville-Thomas, A, Müller, and R. Gaufrés, Reidel, Dordrecht, 1982, p. 17.
17 M. Poliakoff, *J. Chem. Soc., Faraday Trans. 2*, 1977, 569.
18 T. M. McHugh and A. J. Rest, *J. Chem. Soc., Dalton Trans.*, 1980, 2223; R. B. Hitam, R. Narayanaswamy, and A. J. Rest, *ibid.*, 1983, 615; A. Horton-Mastin, M. Poliakoff, and J. J. Turner, *Organometallics*, 1986, **5**, 405.
19 D. C. Andrews and G. Davidson, *J. Chem. Soc., Dalton Trans.*, 1972, 126.
20 W. A. G. Graham, personal communication.
21 D. Sellmann, *Angew. Chem., Int. Ed. Engl.*, 1971, **10**, 919.
22 D. Graham and J. Howard, *Spectrochim. Acta, Part A*, 1985, **41**, 815.
23 H. P. Fritz, *Adv. Organomet. Chem.*, 1964, **1**, 239.
24 I. S. Butler, D. F. R. Gilson, and P. D. Harvey, *Inorg. Chem.*, 1987, **26**, 32.
25 O. Crichton, A. J. Rest, and D. J. Taylor, *J. Chem. Soc., Dalton Trans.*, 1980, 167.

Received 7th June 1989; *Paper* 9/02409C